System Reliability Analysis for Seismic Stability of the Soldier Pile Wall Using the Conditional Random Finite-Element Method

A. R. Kalantari, Ph.D.[1]; and A. Johari[2]

Abstract: The stability of the retaining system under seismic conditions is an important aspect of safe design in earthquake-prone areas. In addition, this stability is highly dependent on soil uncertainty and failure mode contribution. On the other hand, imaging the borehole data directly into the analysis section and ignoring the known data by using unconditional simulation can lead to unrealistic results. Against this background, the current study presents a reliability analysis by incorporating geostatistical conditional simulations and a pseudostatic approach into the Finite-Element Method (FEM) MATLAB code to address the aforementioned issues. Then, the Sequential Compounding Method (SCM) is implemented to calculate the overall system reliability from a combination of the individual subsystem. Reliability analysis of a real case study reveals that compared with the Unconditional Random Finite-Element Method (URFEM), utilizing the Conditional Random Finite-Element Method (CRFEM) helps improve the mean value of the Factor of Safety (FS) against all failure modes by 7%–30%, while reducing the related standard deviation by 12%–43%. The results of system reliability show that bending moment and lateral displacement are the fundamental mechanisms in the static and seismic states. Moreover, implementing conditional simulation in seismic stability analysis offers a 16% and 43% reduction in the mean value and standard deviation of an unsafe distance from the excavation edge, accounting for less uncertainty in the slip surface location. Besides, according to the Coefficient of Variation (COV) of the failure modes, it is concluded that the FS against lateral displacement is chiefly affected by the soil heterogeneity compared with others, while shear force failure mode is less affected.
DOI: 10.1061/(ASCE)GM.1943-5622.0002534.

Practical Applications: Soldier piles are widely used in urban and industrial areas as a temporary or permanent retaining system for constructing underground structures. The stability of the retaining system under seismic conditions is an important aspect of safe design in earthquake-prone areas. In addition, the inherent variability of the soil properties dictates that stability problems are probabilistic rather than deterministic. In the current study, a real case with three boreholes of 22.5 m depth was considered and the soil parameters were estimated via field and laboratory tests. Then, the FS distribution and reliability indices of different failure modes were obtained for both static and seismic states by considering the seismic coefficient and efficient soil properties as stochastic parameters. These curves provided the essential data for structural design based on the target performance level. Next, the variation of the slip surface was determined, which could be used for determining the unsafe zone adjacent to the excavation. The responses of soldier piles indicated that by taking the seismic coefficient into account, the mean value of lateral displacement, maximum shear force, and maximum bending moment increased by 80%, 16%, and 37%, respectively. Moreover, considering different failure modes separately led to an overestimation of the reliability indices by three times.

Author keywords: Pseudostatic finite-element method; Conditional simulation; Soldier pile wall; Random finite-element method; System reliability analysis.

Introduction

Soldier piles are popular retaining systems, typically used for underground systems such as subways. Compared with other retaining systems, the key benefits of soldier piles are low construction time and cost. Hence, the soldier pile wall has become a fascinating topic and has aroused researchers' interest. To evaluate the performance of the soldier pile wall, a consideration of not only soil property uncertainties but also the contribution of different failure modes is essential. It is also crucial to assess the seismic stability of retaining walls, particularly permanent ones in seismic-prone areas.

Because excavation is more vulnerable to seismic loads, especially long-term excavation, the appropriate design of the retaining systems is one of the significant problems encountered in earthquake-prone regions. Despite the extensive use of soldier piles, seismic design guidance documents are inadequate for the safe design of this type of retaining system, even if Eurocode 8 (CEN 2005) presents a guide for the design of retaining walls. The retaining systems' seismic design and analysis procedure can be categorized into three main groups: dynamic, simplified dynamic, and pseudostatic. The pseudostatic method presented by Mononobe (1929), Okabe (1926) to calculate the earthquake-induced lateral earth pressure is relatively simple to implement compared with others. This method makes it possible to apply the seismic acceleration in terms of equivalent static force using the seismic coefficient in the horizontal direction (k_h) as a function of the Peak Ground Acceleration (PGA).

[1]Dept. of Civil and Environmental Engineering, Shiraz Univ. of Technology, Shiraz 7155713876, Iran.

[2]Professor, Dept. of Civil and Environmental Engineering, Shiraz Univ. of Technology, Shiraz 7155713876, Iran (corresponding author). ORCID: https://orcid.org/0000-0002-5988-6964. Email: johari@sutech.ac.ir

Note. This manuscript was submitted on August 21, 2021; approved on April 30, 2022; published online on July 20, 2022. Discussion period open until December 20, 2022; separate discussions must be submitted for individual papers. This paper is part of the ***International Journal of Geomechanics***, © ASCE, ISSN 1532-3641.

Due to the mentioned advantages, the pseudostatic method is widely applied in the retaining walls' seismic design (Bathurst and Cai 1995). Moreover, several researchers tried to develop this method by considering vertical seismic acceleration and other influential aspects of seismic action on the retaining system (Seed and Whitman 1970; Richards and Elms 1979). Choudhury and Ahmad (2007) evaluated the stability of the waterfront retaining wall subjected to pseudostatic earthquake forces. It showed that the FS value was extremely sensitive to the soil and wall friction angle. Smith and Cubrinovski (2011) extended the discontinuity layout optimization method to assess the seismic stability of retaining walls by using the pseudostatic approach. Ruan and Sun (2014) assessed the external seismic stability of geosynthetic-reinforced soil walls in the pseudostatic method framework.

Despite the advantages offered by the pseudostatic method, commonly known as Mononobe–Okabe, this method has some limitations. For instance, the method is incapable of predicting displacement under seismic loading. The pseudostatic FEM offers the tools to overcome these drawbacks. The method is less complicated, costly, and time-consuming than the other dynamic analysis approach and can model in situ stresses prior to seismic loading. Several researchers have used this method to evaluate the seismic performance of geotechnical structures. Rushan and Hongbin (2006) used the finite-element pseudostatic method in the seismic-resistant design of underground structures. Kontoe et al. (2013) evaluated two examples of pseudostatic finite-element analysis and explored the sensitivity of the results on the adopted mesh size. Zou et al. (2017) conducted pseudostatic FEM analysis to predict the nonlinear behavior of underground frame structures subjected to increasing horizontal seismic excitations.

One of the disadvantages of traditional deterministic stability analysis is that the minimum required FS value may not be sufficient for ensuring safety. Moreover, the variation of soil properties is ignored in this method, leading to inappropriate designs. In the early 1970s, a reliability-based method was proposed to aid engineers in making acceptable designs. Some studies have been conducted to evaluate the seismic reliability analysis of the retaining system, but the soldier pile wall has not been given enough consideration. Genske et al. (1991) conducted a reliability analysis of reinforced earth–retaining structures subjected to earthquake loading. Karakostas and Manolis (2002) developed a stochastic numerical analysis for evaluating the dynamic response of underground openings. Basha and Babu (2009) presented the reliability-based load and resistance factor design approach for determining the external seismic stability of reinforced soil walls. GuhaRay and Baidya (2016) proposed design guidelines of gravity retaining walls for different variations of random variables and earthquake conditions in the pseudostatic method framework. Hu et al. (2022) proposed a novel stochastic dynamics method for evaluating the seismic performance of retaining walls. It was found that ignoring the spatial variability of soil properties may overrate the safety of the retaining walls. However, most of these studies do not account for real-site data using an unconditional simulation. Ignoring real data can lead to a conservative design by affecting responses such as internal forces and reliability indices (Gholampour and Johari 2019). Hence, it is of practical importance to take the values and locations of the measured data into consideration in reliability analysis, which can be considered as a useful tool for reducing the degree of uncertainty.

A system consisting of several components can be categorized into two: series and parallel systems (Johari and Fooladi 2020). Because any failure mode of the soldier pile wall will cause the failure of the entire system, it can be represented as a series system. Various failure modes of soldier pile walls are not independent but correlated. A design based on individual failure modes may not satisfy the requirements of other failure modes. Hence, it is crucial to utilize system reliability to consider all failure modes and their correlation. Numerous methods have been presented for determining the overall reliability of systems from the given reliabilities of the components. For instance, Estes and Frangopol (1998) developed a computer program for structural system reliability analysis. It was found that the method provided accurate results for parallel systems with five or fewer components. However, significant errors may result for series systems consisting of components with the same reliability indices. Then, Song and Kang (2009) developed a matrix-based system reliability method. Because the method required many common source random variables to accurately describe the correlation coefficients between components, calculating the overall reliability index was time-intensive. To tackle the shortcomings related to the previous methods, Kang and Song (2010) presented a new method, namely the Sequential Compounding Method (SCM), in which two-component events were compounded sequentially until a single compound event eventually represented the system event. The great benefit of the SCM is that it considers the correlation between components and minimizes logic complexity. Despite the importance of such a retaining system, no work has been reported in the literature on soldier pile walls against all structural and geotechnical failure modes. However, system reliability analysis of other geotechnical problems related to soil nail wall and slope stability has recently been drawing the attention of many researchers (Johari and Rahmati 2019).

To the best of the authors' knowledge, no study that stochastically analyzes the seismic stability of soldier piled walls in the pseudostatic FEM frameworks has been conducted to date. The previous studies did not consider the conditional simulation, structural and geotechnical limit states, a cross-correlation between multiple failure modes, the uncertainty associated with soil properties and the seismic coefficient, and system reliability analysis. This paper aims to tackle these issues via system reliability analysis for ensuring seismic stability of the soldier pile wall by combining the SCM and pseudostatic into the CRFEM, which is the first of its kind. The influences of conditional simulation, seismic state, and system reliability analysis are explained in detail with a distinct comparison between internal forces, deflection, and the reliability index obtained with and without considering these conditions. The effect of conditional simulation on the critical slip surface of the soldier piled wall is also illustrated. For illustrative purposes, an actual excavation with a soldier pile wall is analyzed deterministically in static and seismic conditions using the pseudostatic finite-element-based MATLAB code. Then, reliability analysis is conducted by considering k_h and soil properties as a stochastic parameter using the CRFEM. Next, each failure mode's reliability index is extracted and combined using the SCM to estimate the overall system reliability index. In another part of this paper, the influence of conditional simulation on the statistical parameters of failure modes and unsafe distance from the edge of excavation is also investigated.

Pseudostatic CRFEM Analysis

In this research, a system reliability assessment for determining the seismic stability of the soldier pile wall is presented. In this regard, the geostatistical conditional simulation and pseudostatic are implemented in the FEM to consider the uncertainties related to soil properties and seismic loading for stability analysis. In this way, effective soil properties and k_h are modeled as stochastic parameters, and the numerous failure modes of the soldier pile wall are considered. More details of the implementation procedure are outlined subsequently:

1. Obtaining soil parameters from boreholes and discretizing the domain.
2. Predicting soil parameters on the unsampled levels of boreholes and all levels of imaged boreholes in the section of analysis using the geostatistical method.
3. Generating conditional random fields for determining effective soil parameters.
4. Generating a random variable for k_h.
5. For each element:
   a. Obtaining the total stress using the seismic coefficient and soil unit weight.
   b. Calculating the shear strength.
6. Conducting a pseudostatic FEM strength reduction analysis for determining the FS against global stability and a pseudostatic FEM elastoplastic analysis for estimating the FS against other failure modes.
7. Repeating Steps (2)–(6) for the number of simulations using Monte Carlo Simulation (MCS) to estimate the reliability of failure modes.
8. Extracting the overall system reliability index from individual failure modes.

Finite-Element Modeling of Excavation

The FEM is an effective and powerful reliable numerical technique to analyze complex geotechnical works. Excavation is a complex phenomenon that involves large deformations in which material is removed from the ground. The soil–structure interface varying from perfectly smooth to perfectly rough can be considered in FEM modeling. Because the service load level is lower than that of the failure load, the slippage tends to be small. Hence, implementing interface elements is not significant in displacement assessment (Selvadurai and Boulon 1995). Due to the working load considered in the current study, the perfectly rough condition was modeled for enabling interaction between the soldier piles and the soil.

Details of the finite-element modeling of excavation are provided in the literature (Smith et al. 2013). From an FEM standpoint, all static equilibrium problems take the same form as follows, which can be solved for known forces $\{F\}$ and stiffness $[K]$ to give equilibrium displacements $\{U\}$:

$$\{F\} = [K]\{U\} \tag{1}$$

where each term for a soldier pile wall problem can be expressed as follows:

$$\{F\} = \sum_{i=1}^{ns}(\{F\}_s)_i + \sum_{j=1}^{np}(\{F\}_p)_j \tag{2}$$

$$[K] = \sum_{i=1}^{ns}([K]_s)_i + \sum_{j=1}^{np}([K]_p)_j \tag{3}$$

$$\{U\} = \sum_{i=1}^{ns}(\{U\}_s)_i + \sum_{j=1}^{np}(\{U\}_p)_j \tag{4}$$

where *ns* and *np* are, respectively, the number of soil and pile elements, and indices s and p denote the soil and pile element, respectively.

The nodal force vector consists of two different forces, the body and the external. The gravity forces, which can be categorized as body forces, are given by

$$\{F\}_{\text{gravity}} = \sum_{i=1}^{ns}\left(\gamma\iint[N]^T dxdy\right) \tag{5}$$

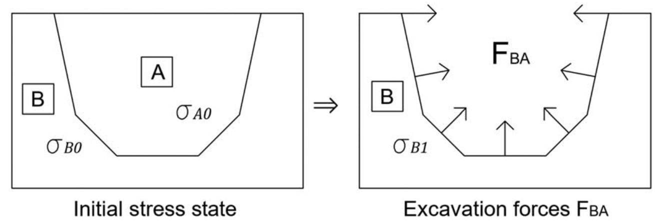

Fig. 1. Formulation of excavation forces.

in which γ is soil unit weight and $[N]$ is element shape function.

This problem mainly differs from the others (e.g., slope stability) in the sense that an equal force must be exerted on the boundary, as illustrated in Fig. 1. The excavation force (F_{BA}) exerted on an excavation surface, which is affected by self-weight and the stress state of excavated material (σ_{A0}), can be estimated as follows (Smith et al. 2013):

$$\{F_{\text{BA}}\} = \int_{V_A}[B]^T\{\sigma_{A0}\}dV_A + \gamma\int_{V_A}[N]^T dV_A \tag{6}$$

where $[B]$ = strain–displacement matrix; and V_A = excavated volume.

Pseudostatic Analysis

The pseudostatic method can be classified into two categories, namely, force and deformation based. In the first one, which is used in the current work, the earthquake-induced load is implemented as a constant body force perpendicular to each other in the main axes of the coordinates:

$$F_h = k_h W \tag{7}$$

$$F_v = k_v W \tag{8}$$

where F_h and F_v = body forces in the X- and Y-directions; k_h and k_v = corresponding seismic coefficients; and W = weight of the failure mass.

Geostatistics

An evaluation of uncertainty is vital for those problems that involve significant interaction with earth materials. In geotechnical applications, engineers estimate soil parameters based on limited data obtained through a site investigation and through laboratory tests. Geostatistical approaches provide a framework for implementing the specific *known* properties and modeling the uncertainty associated with soil properties (Rouhani et al. 1996). The main aim of implementing the geostatistical technique is to estimate the soil parameters between known data, which usually consist of samples representing a scarce portion of the total volume of soil (Parsons and Frost 2002).

Semivariogram Analysis

Estimating the correlation between samples along a specific orientation is an essential requirement in most geostatistic applications, which is generally done by modeling the semivariogram. The experimental semivariogram for a set of data $Z(x_i)$, $i = 1, 2, \ldots$ can be defined as follows (Webster and Oliver 2007):

$$\gamma_{jj}(h) = \frac{1}{2N_{jj}(h)} = \sum_{i=1}^{N} [Z_j(X_i) - Z_j(X_i + h)]^2 \tag{9}$$

where $N_{jj}(h)$ = number of pairs of data points separated by the particular lag vector h. The cross-semivariogram for random functions $Z_j(x)$ and $Z_k(x)$, which describes the spatial dependence between cross-correlated variables, can be achieved as follows:

$$\gamma_{jk}(h) = \frac{1}{2N_{jk}(h)} = \sum_{i=1}^{N} \{[Z_j(x_i) - Z_j(x_i + h)][Z_k(x_i) - Z_k(x_i + h)]\} \tag{10}$$

where $N_{jk}(h)$ is the number of pairs of data points, separated by h, which have measured values of both random function $Z_j(x)$ and $Z_k(x)$.

Kriging and Cokriging Interpolation

The Kriging method is a precise interpolation estimator used as a univariate geostatistical tool to find the values at unsampled locations by a weighted averaging of nearby samples. However, multivariate geostatistical analysis is used to evaluate two or more co-regionalized variables (i.e., regionalized variables that display cross-correlation). The Cokriging method can be applied in this kind of analysis to consider the cross-correlation and autocorrelation (Matheron 1963). The unique application of Cokriging is to decrease estimation variances where one or more of the regionalized variables (i.e., random variables with space coordinates) are *undersampled* and correlated with each other. Undersampling refers to a circumstance in which the number of the primary variable to be estimated (e.g., shear strength parameters) is much smaller than the others (e.g., unit weight), usually at a subset of the sampling points.

Conditional Simulation

If soil properties are known at particular locations, conditional simulation should be utilized to make sure that the simulated random field matches the data at these locations exactly. An unconditional simulation ignores this known data and will cause considerable variability in the response quantities. Conditional simulation techniques can be classified into two categories, namely indirect and direct approaches. Indirect approaches are based on unconditional simulation, transformed into conditional ones. These approaches are employed when the mean (μ) and variance are known and constant over the region of interest. However, direct approaches are employed when the mean and variance are unknown or variable. Further details on the conditional simulation can be found in (Griffiths and Fenton 2007).

System Reliability Approach

An identification of system components (i.e., failure modes) can be regarded as the primary step to conducting system reliability analysis. The reliable design of retaining systems mainly includes three limit states: (1) external stability; (2) serviceability; and (3) structural (Luo et al. 2018). These can be subdivided into various failure modes with different significance levels depending upon the parameters, such as neighboring existing structures and excavation depth.

The external stability of retaining systems consists of two components: the global failure and the sliding failure mode. The second component is often ignored in the soldier pile wall due to enough stabilizing force. In this study, the global stability, which represents with (FS_G), is obtained by performing the finite-element strength reduction analysis.

One of the significant problems facing excavation in an urban region is the risk of damage to neighboring buildings caused by the excavation-induced lateral wall deflection. Hence, the soldier pile wall's maximum lateral deflection is the primary failure mode of the serviceability limit state. To prevent damage to adjacent buildings, the limiting value of lateral deflection is taken as 0.65% of the excavation depth based on the findings of Ali and Khan (2017).

Because the axial force in soldier piles is relatively small compared with other internal forces, the structural limit state can be categorized as shear force and bending moment failure mode.

For representing failure modes against shear force (FS_{SF}), bending moment (FS_{BM}), and lateral displacement (FS_{LD}), performance functions are defined as follows:

$$\mathrm{FS} = \frac{R}{L} \tag{11}$$

where R = failure force or limiting lateral displacement; and L = maximum excavation-induced force or lateral displacement obtained from the elastoplastic analysis.

Implementation Procedure of Stability Analysis

Previous sections described the processes for pseudostatic FEM modeling of excavation, obtaining the FS against various failure modes, generating conditional simulation, and performing system reliability analysis. The central focus of this section is on implementing the presented seismic system reliability analysis for the soldier pile wall.

Case Study

An actual case study of the soldier pile wall is considered to evaluate the presented method's efficiency and validation of the coded program. To do this, deterministic analysis is pursued by a

Fig. 2. Satellite overview of site location. (Image © Google, Imagery ©2022 CNES/Airbus, Maxar Technologies, Map data ©2022.)

Fig. 3. Soldier pile wall of the studied site.

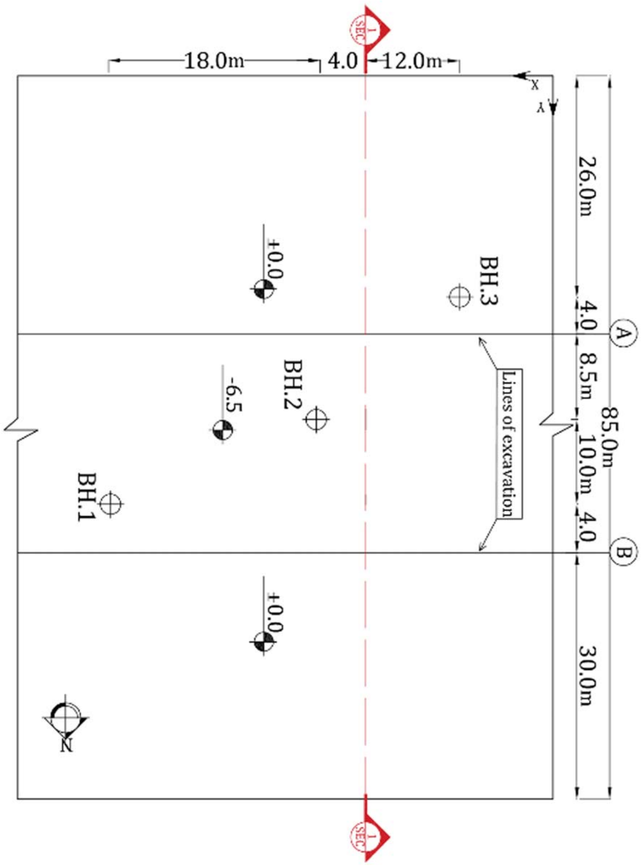

Fig. 4. Relative location of the boreholes.

reliability assessment to include the variation of soil properties and the seismic coefficient. Then, system reliability analysis was performed to compute a single reliability index for the entire soldier pile wall system.

Site Characteristics

The actual case study employed in this paper, constructed in 2020 for the purposes of transportation system improvement, is a soldier pile wall in the city of Shiraz, located in the southwest of Iran, as

Table 1. Site soil properties from BH.1 to BH.3

	BH.1						BH.2						BH.3					
Depth (m)	Type	SPT value	Unit weight (kN/m^3)	Friction angle (Deg.)	Cohesion (kN/m^2)	Modulus of elasticity (kN/m^2)	Type	SPT value	Unit weight (kN/m^3)	Friction angle (Deg.)	Cohesion (kN/m^2)	Modulus of elasticity (kN/m^2)	Type	SPT value	Unit weight (kN/m^3)	Friction angle (Deg.)	Cohesion (kN/m^2)	Modulus of elasticity (kN/m^2)
2.5	CL-ML	23	18.83	21.9	22.1	18,000	CL-ML	21	18.34	22.3	20.8	19,000	CL	19	19.23	—	—	19,500
5.0	CL-ML	19	18.74	—	—	17,500	CL	20	18.44	21.9	21.6	16,000	CL	21	19.52	21.9	23.9	18,000
7.5	CL	27	19.72	22.9	24.9	20,000	CL-ML	28	18.64	—	—	19,000	CL-ML	28	19.62	23.1	22.8	21,000
10.0	SP-SM	35	20.40	31.6	12.2	28,000	GM	37	18.74	—	—	31,000	GM	39	20.11	33.9	14.3	32,000
12.5	GP	49	20.71	34.8	12.4	45,000	GM	50	18.93	34.9	12.0	40,000	GM	48	20.50	—	—	45,000
15.0	GP	55	20.70	—	—	49,000	GM	53	19.23	—	—	45,500	GM	50	20.70	—	—	46,500
17.5	GM	65	19.82	—	—	53,000	GC	62	19.33	36.6	13.5	51,000	GM	61	20.89	36.9	12.1	53,500
20.0	GM	70	20.21	36.8	12.0	57,500	GM	69	19.72	—	—	57,000	GC	70	20.90	—	—	56,000
22.5	GP	75	20.60	—	—	61,000	GM	78	20.01	36.9	13.0	62,500	CL	67	21.09	29.6	18.2	65,000

depicted in Fig. 2. The soldier pile wall consists of 12.0- m-high cast-in-place reinforced concrete piles embedded 5.0 m below the final excavation level. After placing the soldier piles, excavation is carried out to the basement level without any support system such as a strut. The main aim of selecting the site is that it is located in an earthquake-prone area. Besides, the whole domain of the soldier pile wall satisfies the generalized plane strain conditions, as shown in Fig. 3.

Site Soil Properties

To obtain soil properties, three boreholes (i.e., BH.1–BH.3) with 22.5- m depth from the ground surface are drilled. The location and number of boreholes are determined based on the Iranian geotechnical code (BHRC 2014a). The relative location of the real boreholes is illustrated in Fig. 4. Soil properties such as Poisson's ratio (v), modulus of elasticity (E_S), cohesion (c), friction angle (φ), and unit weight (γ) are specified by field tests [e.g., the Standard Penetration Test (SPT)] and laboratory tests (e.g., grain size analysis, particle density, Atterberg limit tests). Based on the site and laboratory investigations, a value of 2.68 g/cm^3 is obtained for particle density. Soil parameters of BH.1 to BH.3 are presented in Table 1. As can be seen, the soil profile of the studied site mainly consists of two layers. The fine-grained soil is encountered from the ground surface to a depth of 7.5 m, and the coarse-grained soil is located between 10.0 and 22.5 m. It is notable that v is obtained according to the typical values suggested by Bowles (1988), and E_S is obtained using the correlations between the geotechnical parameters and the SPT results proposed for the city in the case study (Behpoor and Ghahramani 1989).

Modeling and Verification

An FEM MATLAB code is developed to evaluate the FS against failure modes under static and seismic conditions. The code is for the two-dimensional, plane strain analysis of elastic-perfectly plastic soils with a Mohr–Coulomb failure criterion and a nonassociated flow rule. The soldier piles and soil are modeled, respectively, with a two-noded 1-D rod-beam and eight-node quadrilateral elements. Determining model dimensions and predicting soil parameters in the analysis section are the key steps in FEM modeling, as described in the following subsections.

Determination of Model Dimensions

Precision and effectiveness are the two main concerns in FEM modeling. Although enlarging the model's dimensions cannot significantly improve the precision of the results, it increases computation time. In stochastic analysis, the process is rendered somewhat complicated because it is repeated multiple times. Therefore, a sensitivity analysis is required to assess the effect of the model dimensions on the results. For this purpose, the problem was modeled with different dimensions, as presented in Table 2. Also, the properties of the soldier piles and soil implemented in the analysis are tabulated in Tables 3 and 4, respectively. The $k_h = 0.15$ was selected as half of the PGA, based on Iranian geotechnical and seismic design codes (BHRC7, BHRC 2014a; BHRC2800, BHRC 2014b). The results of the dimension sensitivity analysis are shown in Figs. 5(a and b) for the static and seismic states, respectively. It was observed that the variation of the FSs changed before and after Case No. 5. Therefore, Case No. 5 was selected as a model geometry due to its efficiency. Besides, all dimensions of the selected case were compared with the values proposed by Brinkgreve et al. (2014) to verify the model geometry.

Verification of the Coded Program

The general conditions of the model are presented in Fig. 6 through cross sections 1-1 of Fig. 4. Also, the related finite-element mesh is shown in Fig. 7. With regard to boundary conditions, the bottom boundary was restrained against the translational degree of freedom in the X- and Y-directions, while the side boundaries were allowed to move only in the vertical direction.

The value of the FS against all failure modes in deterministic analysis with and without considering seismic conditions is reflected in Table 5. As was expected and reported before (Li et al. 2006), implementing the seismic condition in stability analysis led to a lower value of FSs.

A comparison of the deterministic analysis results with the results obtained from FLAC 7.0 software was made under static and seismic conditions to verify the program. To do this, geometry with the same properties mentioned in the previous subsection was modeled with a developed program and FLAC. As illustrated in Fig. 8 for lateral displacement and Table 6 for all responses, commercial software results are close to those from the developed program.

Stochastic Analysis

In this section, the stochastic analysis of the selected case study is outlined in subsections. First, a sensitivity analysis is presented to determine effective soil parameters for the stochastic analysis of the soldier pile wall. Second, CRFEM and URFEM analyses are offered to evaluate the effect of conditional simulation on the statistical parameters of failure modes. Finally, the sensitivity

Table 2. Input values for determination of the model dimension

Case no.	Dimension (m × m)
1	34 × 22
2	37 × 24
3	41 × 26
4	45 × 28
5	50 × 30
6	55 × 32

Table 4. Parameters of soils used in FEM analysis

Layer	Unit weight (g/cm^3)	Friction angle (Deg.)	Cohesion (kPa)	Modulus of elasticity (kPa)	Poisson's ratio
1	19.0	22.7	22.3	18,500	0.35
2	20.1	34.7	13.3	48,000	0.25

Table 3. Parameters of soldier piles used in FEM analysis

Diameter (m)	Space (m)	f'_c (MPa)	EI (kN.m^2)	EA (kN)	Unit weight (kN/m^3)	Poisson's ratio	Shear capacity (kN)	Moment capacity (kN.m)
1.0	2.2	25	631,273	9,223,750	23.80	0.10	390	295

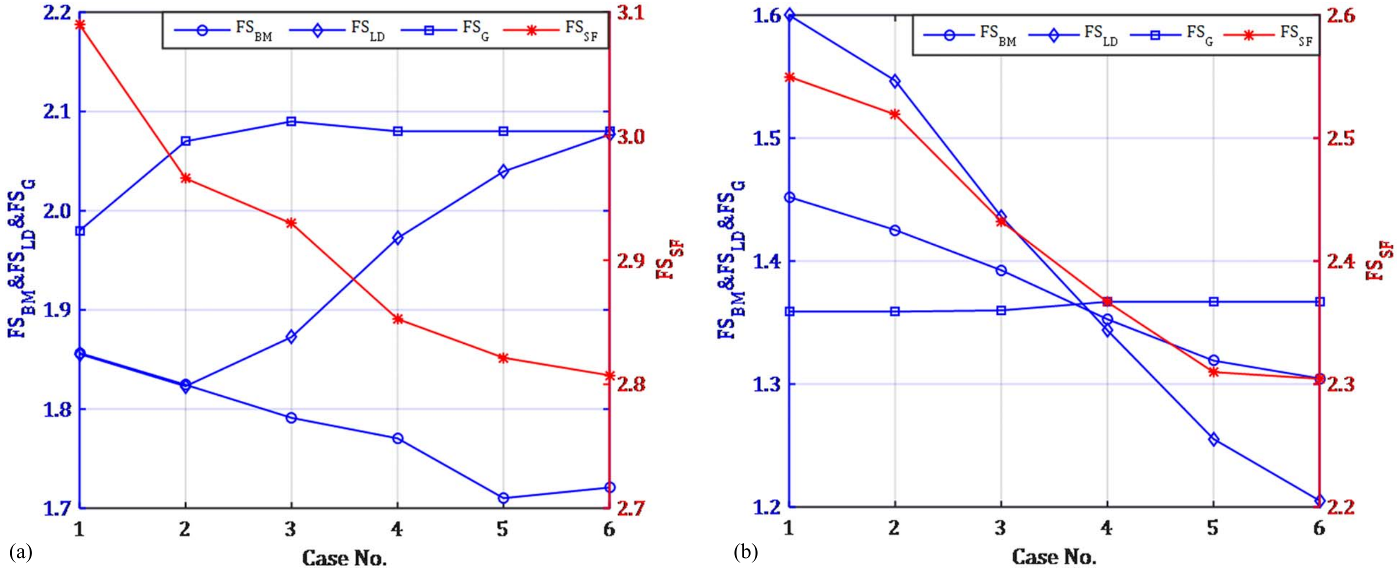

Fig. 5. Dimension sensitivity analysis: (a) static state; and (b) seismic state.

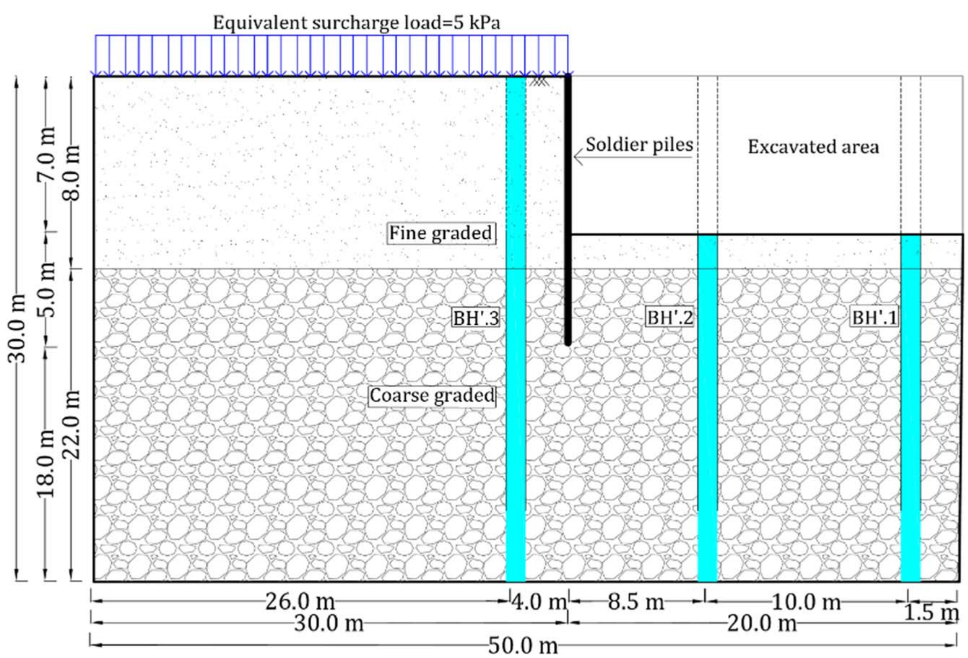

Fig. 6. Cross section 1-1 of Fig. 7.

analysis is presented to estimate the optimal number of realizations.

Sensitivity Analysis for Selecting Effective Soil Parameters

Identifying the effective parameters can be considered the first step of stochastic analysis. To do this, a sensitivity analysis was performed and the importance of input parameters for all failure modes was determined, as shown in Table 7. For this purpose, each parameter was increased by 10% of its value, while other input parameters were kept constant. It was observed that the order of importance of input parameters changed with the failure modes. Also, γ, c, φ, and E_S were the most influential parameters on the safety factors, while Poisson's ratio had no significant effect.

Stochastic Analysis of Soldier Pile Wall by URFEM

The unconditional random fields were generated for effective soil parameters selected based on the sensitivity analysis. The seismic acceleration's vertical component was ignored because its effect on earthquake-induced permanent displacements is generally not relevant and believed to be relatively minor (Bray et al. 2010).

The stochastic parameters were modeled within three standard deviations (σ) of difference from the μ, using truncated normal probability distribution functions with the μ and σ tabulated in Table 8, determined from known data presented in Table 1. The correlation coefficient between shear strength parameters was selected $\rho_{c,\varphi} = -0.5$ based on previous studies (Cherubini 2000). Furthermore, the correlation lengths were considered 10 and 2.5 m in the X- and Y-directions due to the fact that the horizontal correlation was

Int. J. Geomech., 2022, 22(10): 04022159

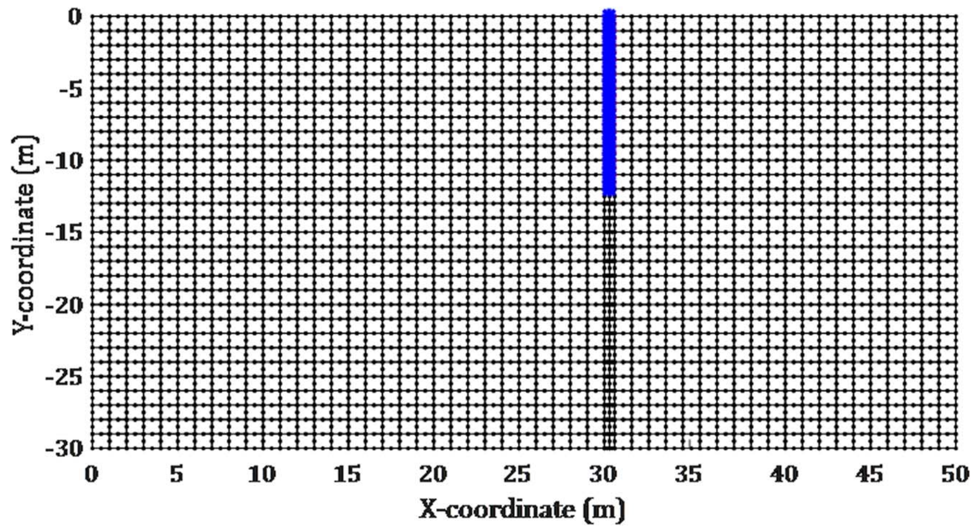

Fig. 7. Finite-element mesh.

Table 5. Value of FS for various failure modes in the deterministic analysis

Failure mode	Static state	Seismic state
FS_{BM}	1.78	1.30
FS_{SF}	3.29	2.83
FS_{LD}	2.28	1.21
FS_{G}	1.92	1.52

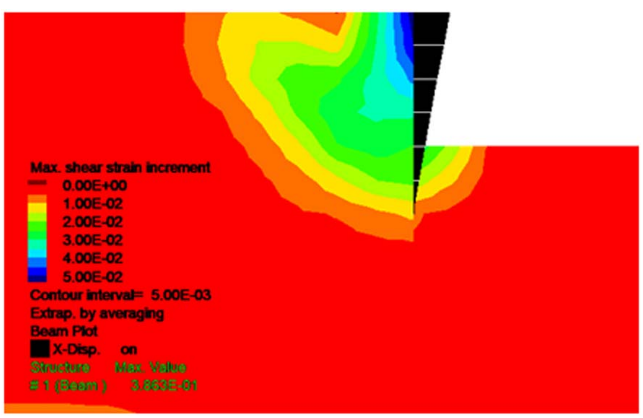

Fig. 8. Soldier piles lateral displacement estimated by using FLAC.

Table 6. Comparison of the soldier pile responses

Models	State	Maximum lateral displacement (mm)	Maximum shear force (kN)	Maximum bending moment (kN·m)
Proposed	Static	19.7	118.6	165.4
model	Seismic	37.1	137.7	226.4
FLAC	Static	20.8	119.3	164.2
	Seismic	38.0	138.4	225.1

much greater, and its impact is generally significantly smaller than the vertical ones (Phoon and Kulhawy 1999). More details about the unconditional random field generation are provided in (Griffiths and Fenton 2007). The unconditional simulation of stochastic parameters through one realization is depicted in Figs. 9(a–d).

Table 7. Sensitivity analysis for selecting the effective input parameters

Failure mode	FS_G	FS_{BM}	FS_{SF}	FS_{LD}
Order of importance of input parameters	γ	φ	φ	E_S
	c	γ	γ	γ
	φ	E_S	c	φ
	E_S	c	E_S	c
	ν	ν	ν	ν

Table 8. Statistics of soil properties for unconditional simulation

Parameters	Distribution	Mean (μ)	Standard deviation (σ)
Modulus of elasticity (kPa)	Normal	39,000	16,000
Cohesion (kPa)	Normal	17.05	5.07
Friction angle (Deg.)	Normal	29.7	6.56
Unit weight (kN/m^3)	Normal	19.7	0.84
k_h	Exponential	0.15	0.02

Stochastic Analysis of Soldier Pile Wall by CRFEM

The geostatistical approach is utilized to maintain the actual fluctuation of soil parameters between the known data at particular locations. To achieve this, and to overcome the disadvantages of unconditional simulation, such as unconformity of measured and simulated values in sampled points, the conditional simulation for effective parameters (i.e., γ, c, φ, and E_S) was generated through geostatistical analysis.

As the first step of the geostatistical analysis, a regression analysis was conducted between all pairs of stochastic parameters to evaluate the dependency of the parameters. Based on the results, the shear strength parameters (i.e., c and φ) of the evaluated soil samples show high dependency on each other. Hence, the Cokriging method was employed to assess the shear strength parameters, and the other parameters were assessed using the Kriging method. The Cokriging method for shear strength parameters improves reliability analysis efficiency, which can be counted as one of its advantages. Because determining the shear strength is much more costly and time-consuming than determining other soil properties (e.g., unit weight), the number of known data is limited in a site investigation. To overcome this limitation, the Cokriging method was utilized to improve the interpolation evaluation

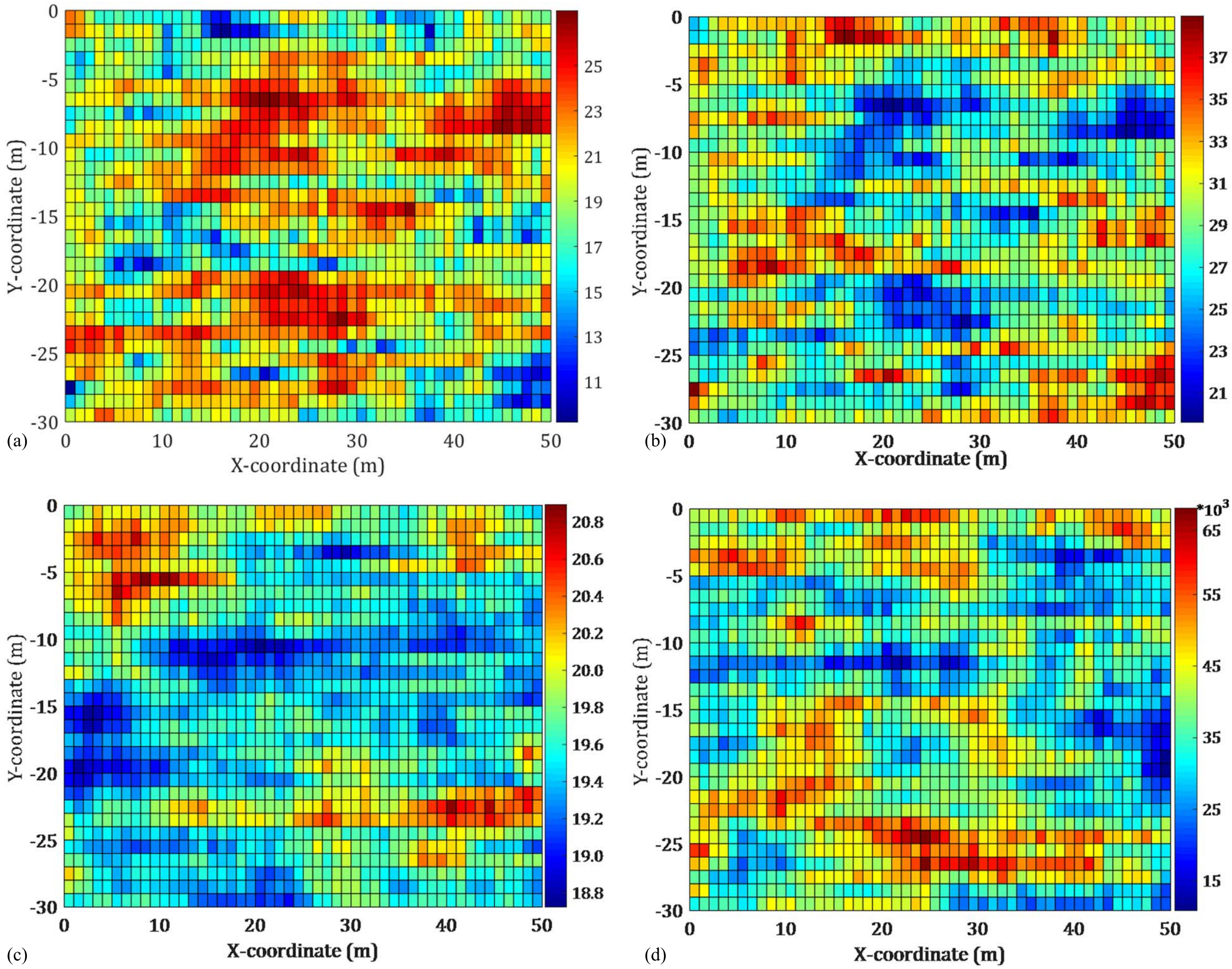

Fig. 9. Sample unconditional simulation of spatial variation for the (a) cohesion (kN/m^2); (b) friction angle (Deg.); (c) unit weight (kN/m^3); and (d) modulus of elasticity (kN/m^3).

without doing more intense sampling, which can be considered as the other reason for using this method.

However, the data in a geotechnical project are generally available in one specific direction, and the amount of data is too small to cover a vast area of the site. More intensive field tests are needed to make an appropriate correlation from the site investigation data. Contrary to the conventional unconditional random fields in which the scale of fluctuation is obtained from known data, in the current approach, this factor is estimated using anisotropy semivariogram analysis of the available data in any direction, which is one of the advantages of the geostatistical method.

The conditional prediction of soil properties in the current study mainly consists of three steps and can be described as follows:

1. Determining the data of the unsampled location of boreholes by interpolation between known data, as shown, for example, in Fig. 10(a) for a depth of 7.5 m of BH.2.
2. Predicting soil properties at each level of imaged boreholes in a section of analysis using the boreholes' soil properties at the same level. An example is shown in Fig. 10(b) for BH′.1.
3. Estimating the soil properties of each element in a section of analysis by considering the soil properties of imaged boreholes as a known data.

The prediction of soil parameters in unsampled locations and imaged boreholes is tabulated in Tables 9 and 10, respectively. The conditional simulation of stochastic parameters through one realization is depicted in Figs. 11(a–d). From these figures, it is seen that cohesion has an inverse relation with friction angle. Moreover, the simulated random fields match the known data at sampled locations, accounting for the differences between the conditional and the unconditional simulations. In the conditional simulation, the random field at measured locations of the domain is constant in each realization, while the rest of the domain is stochastic. However, in the unconditional simulation, the random field at any domain location changes randomly from one realization to another. Hence, the conditional simulation yields much smoother and continuous random fields.

Estimating the Optimal Number of Realizations

The FSs give a quantitative evaluation of stability against different failure modes. The obtained values of the FSs are never absolutely precise due to the uncertainty of quantities involved in the evaluation of the FSs. To conduct a reliability analysis, the CRFEM and URFEM steps were repeated as required to obtain the Probability

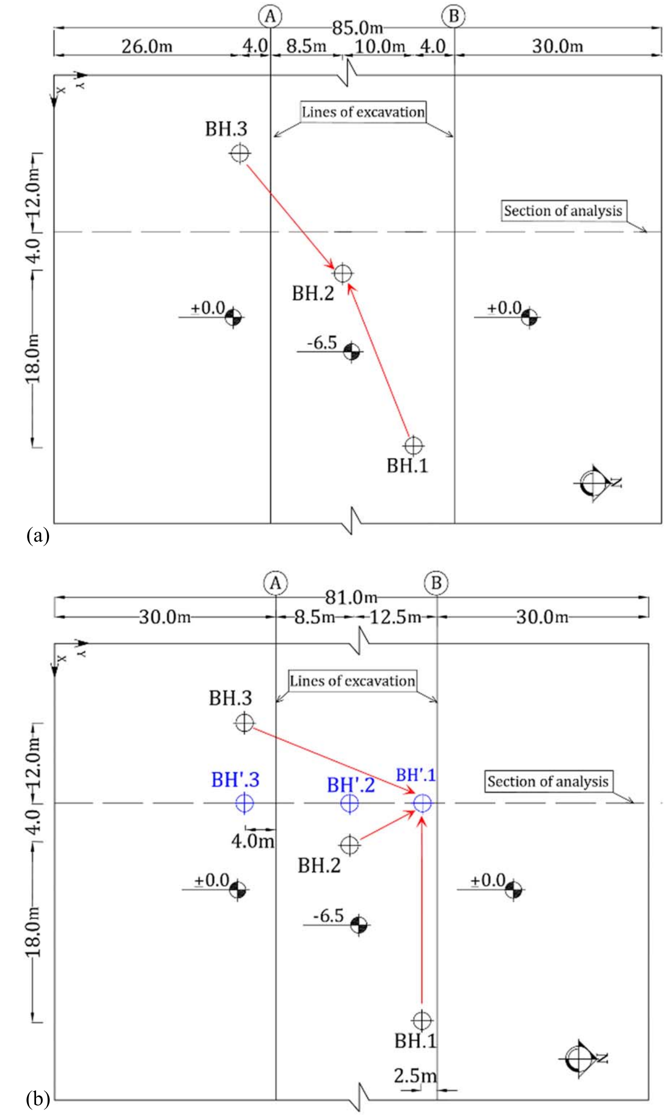

Fig. 10. Prediction of soil parameters in the (a) unsampled level (e.g., depth 7.5 m of BH.2); and (b) imaged boreholes (e.g., BH′.1).

Density Function (PDF) of the FS against all failure modes of the soldier piles. The number of realizations required for any reliability analysis is a function of the required accuracy of the results; the more the number of realizations, the more accurate the predictions are. However, increasing the number of realizations beyond a specific limit will lead to little or no improvement in the accuracy of the analysis. Recent research (Rahman and Nguyen 2012) used statistical parameters to estimate the essential number of simulations, such as μ, σ, and the COV, which is defined as the ratio of the σ to the μ. In the current research, a sensitivity analysis was performed using a COV of the FS against all failure modes. Fig. 12 shows the variations of the estimated COV of FSs with the number of realizations in the static state. The optimum number of simulations was determined to be 500, beyond which no further variation occurred in the value of COVs.

Results and Discussion

This section presents the stochastic responses of the soldier pile wall induced by excavation and the seismic effects in several

Table 9. Prediction of soil parameters in the unsampled locations

Depth (m)	BH.1 Type	Unit weight (kN/m^3)	Friction angle (Deg.)	Cohesion (kN/m^2)	Modulus of elasticity (kN/m^2)	BH.2 Type	Unit weight (kN/m^3)	Friction angle (Deg.)	Cohesion (kN/m^2)	Modulus of elasticity (kN/m^2)	BH.3 Type	Unit weight (kN/m^3)	Friction angle (Deg.)	Cohesion (kN/m^2)	Modulus of elasticity (kN/m^2)
2.5	CL-ML	18.83	21.9	22.1	18,000	CL-ML	18.34	22.3	20.8	19,000	CL	19.23	**22.2**	**23.4**	19,500
5.0	CL-ML	18.74	**22.3**	**21.7**	17,500	CL	18.44	21.9	21.6	16,000	CL	19.52	21.9	23.9	18,000
7.5	CL	19.72	22.9	24.9	20,000	CL-ML	18.64	**25.8**	**19.1**	19,000	CL-ML	19.62	23.1	22.8	21,000
10.0	SP-SM	20.40	31.6	12.2	28,000	GM	18.74	**30.5**	**14.7**	31,000	GM	20.11	33.9	14.3	32,000
12.5	GP	20.71	34.8	12.4	45,000	GM	18.93	34.9	12.0	40,000	GM	20.50	**32.3**	**13.9**	45,000
15.0	GP	20.70	**33.7**	**16.7**	49,000	GM	19.23	**35.4**	**14.2**	45,500	GM	20.70	**33.8**	**13.8**	46,500
17.5	GM	19.82	**35.2**	**16.7**	53,000	GC	19.33	36.6	13.5	51,000	GM	20.89	36.9	12.1	53,500
20.0	GM	20.21	36.8	12.0	57,500	GM	19.72	**36.6**	**13.7**	57,000	GC	20.90	**33.2**	**15.2**	56,000
22.5	GP	20.60	**35.6**	**15.4**	61,000	GM	20.01	36.9	13.0	62,500	CL	21.09	29.6	18.2	65,000

Note: The bold numbers are predicted by using the geostatistical method in unsampled locations

Table 10. Prediction of soil parameters in the imaged boreholes BH′.1 to BH′.3

	BH′.1					BH′.2					BH′.3				
Depth (m)	Type	Unit weight (kN/m^3)	Friction angle (Deg.)	Cohesion (kN/m^2)	Modulus of elasticity (kN/m^2)	Type	Unit weight (kN/m^3)	Friction angle (Deg.)	Cohesion (kN/m^2)	Modulus of elasticity (kN/m^2)	Type	Unit weight (kN/m^3)	Friction angle (Deg.)	Cohesion (kN/m^2)	Modulus of elasticity (kN/m^2)
2.5	CL-ML	18.64	22.1	21.9	18,900	CL-ML	18.59	22.3	21.7	19,100	CL	18.64	22.3	22.1	19,300
5.0	CL-ML	18.54	23.1	20.2	16,900	CL	18.44	21.9	22.2	16,800	CL	18.45	21.9	22.4	17,300
7.5	CL	18.74	23.8	22.9	19,900	CL-ML	18.93	24.9	20.1	19,800	CL-ML	18.89	24.7	20.9	20,300
10.0	SP-SM	19.62	31.4	13.8	30,600	GM	19.13	31.8	14.6	30,800	GM	19.23	31.8	14.4	31,100
12.5	GP	20.01	34.6	12.6	42,900	GM	19.82	34.1	13.3	42,400	GM	19.91	33.8	13.8	43,400
15.0	GP	20.11	34.6	14.1	46,900	GM	19.91	35.0	12.8	46,100	GM	19.62	35.1	13.9	46,800
17.5	GM	19.72	35.9	15.2	52,100	GC	19.92	36.7	13.0	51,800	GM	19.82	36.7	13.0	52,500
20.0	GM	20.11	36.2	12.6	57,000	GM	20.11	35.5	14.1	56,800	GC	20.11	35.5	14.1	56,500
22.5	GP	19.82	34.5	15.1	62,600	GM	19.72	34.3	15.4	62,900	CL	19.52	30.8	15.5	63,800

subsections. First, the seismic effects on soldier pile wall responses are investigated. Then, the influence of geostatistical conditional simulation on soldier piles' responses and slip surfaces is evaluated by comparing the results of the CRFEM with the conventional URFEM analysis.

Effects of Seismic Condition on Soldier Piles' Responses

CRFEM and URFEM analyses were conducted with and without considering the seismic state to assess the effect of the seismic condition on different failure modes. The seismic coefficient was ignored in the static condition, and 500 random fields were generated for stochastic parameters. However, in the seismic assessment, analyses were performed by considering all stochastic parameters because of the crucial role of seismic conditions in the stability of the retaining systems. The variations of the soldier piles' responses by a good fit of the lognormal distribution are presented in Figs. 13(a–c) for the static and seismic conditions of the CRFEM analysis. It shows the importance of determining the best fit for the distribution of responses, which has been ignored in some previous literature by choosing the same distribution type as random input variables. As can be seen, the mean value of the internal forces is smaller than the magnitude in the deterministic case. In other words, the effective soil strength parameters in spatially varied soils are smaller than those in homogeneous soil. Here, effective soil strength parameters mean the overall soil strength parameters of a spatially varied soil within the soil domain. It is observed that, by taking the seismic coefficient into account, the mean value of lateral displacement, maximum shear force, and maximum bending moment increases by 80%, 16%, and 37%, respectively. Besides, the seismic state increases the standard deviation of the lateral displacement, maximum shear force, and maximum bending moment by 3.11, 1.32, and 2.25 times, respectively.

In order to compare the failure probability of the static and seismic states, the Cumulative Density Functions (CDFs) of the FS against all failure modes are illustrated in Figs. 14(a–d). As can be seen, considering seismic condition shift the CDF of FS with respect to some failure mode (e.g., FS_{LD}) from safe to hazardous zone based on USACE (1997). These figures indicate that ignoring the seismic condition can lead to an unsafe design of retaining systems.

These CDFs can also be used to utilize reliability analyses in structural design. Calculating the essential data for structural design mainly comprises three steps, and each step is briefly introduced here. First, specify the P_f to achieve the target performance level, which is presented in the US Army Corps of Engineers (USACE 1997). Then, calculate the FS corresponding to P_f using the related CDF. For instance, as shown in Fig. 14(d), the FS_{BM} corresponding to $P_f = 50\%$ for the URFEM analysis in the static and seismic states is 1.05 and 1.38, while these values increase to 1.29 and 1.68 for the CRFEM. Finally, the design force or displacement is estimated by knowing the failure force and limiting the lateral displacement of the soldier piles.

The statistical parameters and reliability index (β) of different failure modes are presented in Table 11. The β, which is an alternative measure of safety, for lognormal distributed PDF of the FSs can be defined as follows:

$$\beta = \frac{\ln\left[\mu/\left(\sqrt{1+\mathrm{COV}^2}\right)\right]}{\sqrt{\ln\left(1+\mathrm{COV}^2\right)}} \tag{12}$$

As can be seen, among the failure modes' reliability indices, the most critical one is related to bending moment and lateral displacement in the static and seismic conditions, respectively. Besides, the

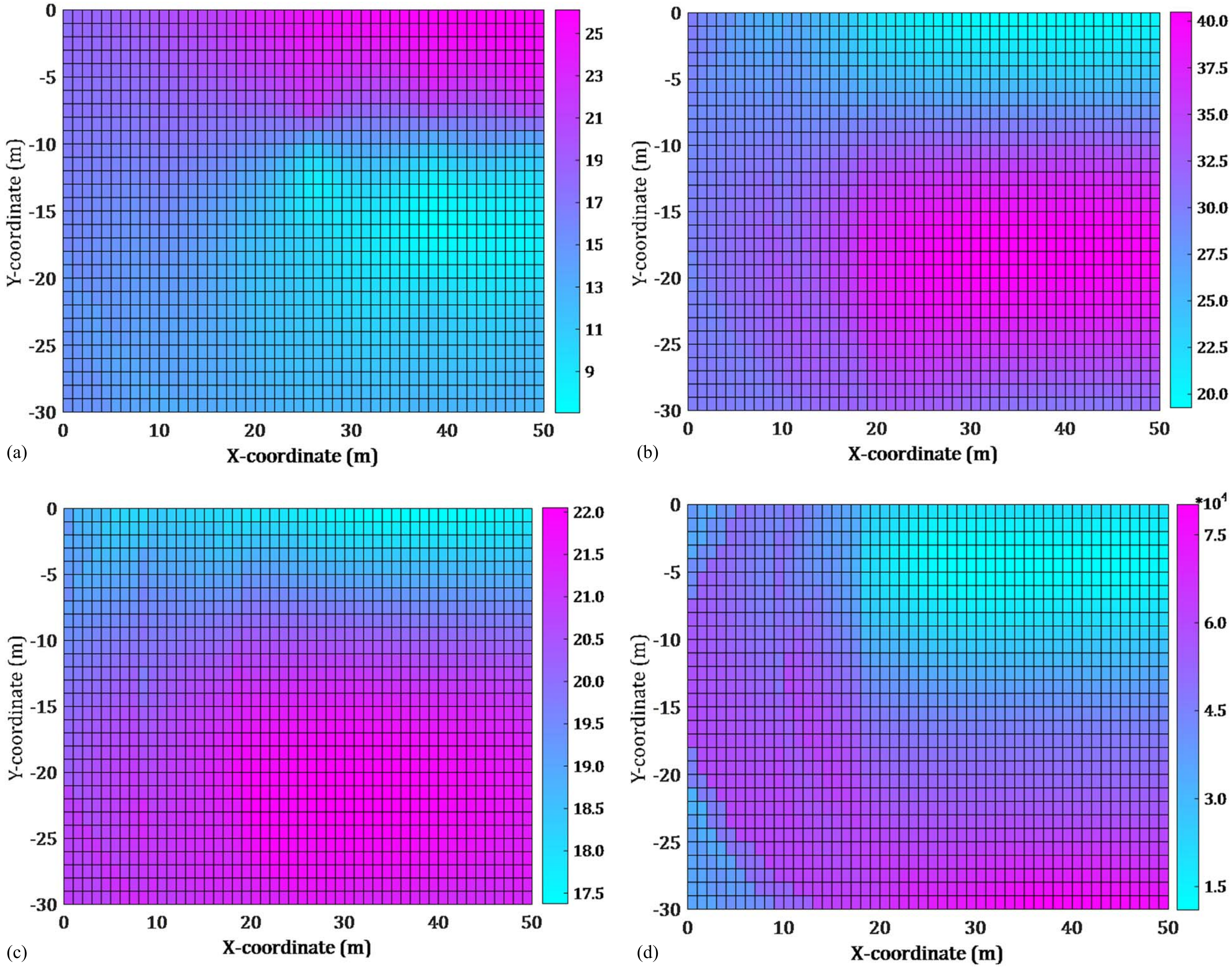

Fig. 11. Sample geostatistical conditional simulation of spatial variation for the (a) cohesion (kN/m^2); (b) friction angle (Deg.); (c) unit weight (kN/m^3); and (d) modulus of elasticity (kPa).

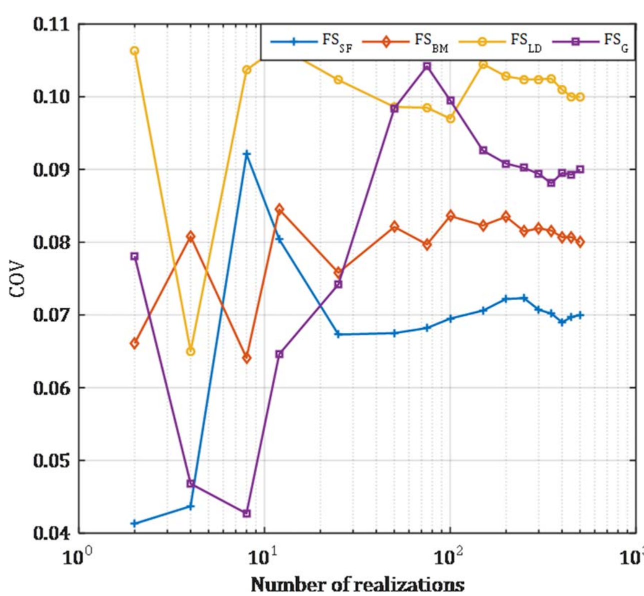

Fig. 12. Variation of COV with the number of realizations.

FS_{SF} has the highest reliability index in both the static and the seismic states. Based on the presented COV of the failure modes in both states, it can be observed that the uncertainty of soil properties has the most important influence on the FS_{LD}, while FS_{SF} is less affected than the others.

Effects of Conditional Simulation on Soldier Piles Responses

To investigate the effect of the geostatistical conditional simulation, the CDFs of FS against all failure modes were extracted by using both CRFEM and URFEM analyses. The statistics and probabilistic properties of these CDFs for both methods are tabulated in Table 11. The standard deviation of all CDFs based on the CRFEM analysis decreases compared with the value obtained from the URFEM analysis. This indicates that the values of the FS are not widely dispersed around the average, which can be considered as an aim of reliability analysis. In the CRFEM analysis, the standard deviation decreases, and the mean value of the FS increases, as illustrated in Figs. 14(a–d). These considerable variations cause different results in reliability analysis outcomes. A comparison of the reliability indices obtained by the two methods

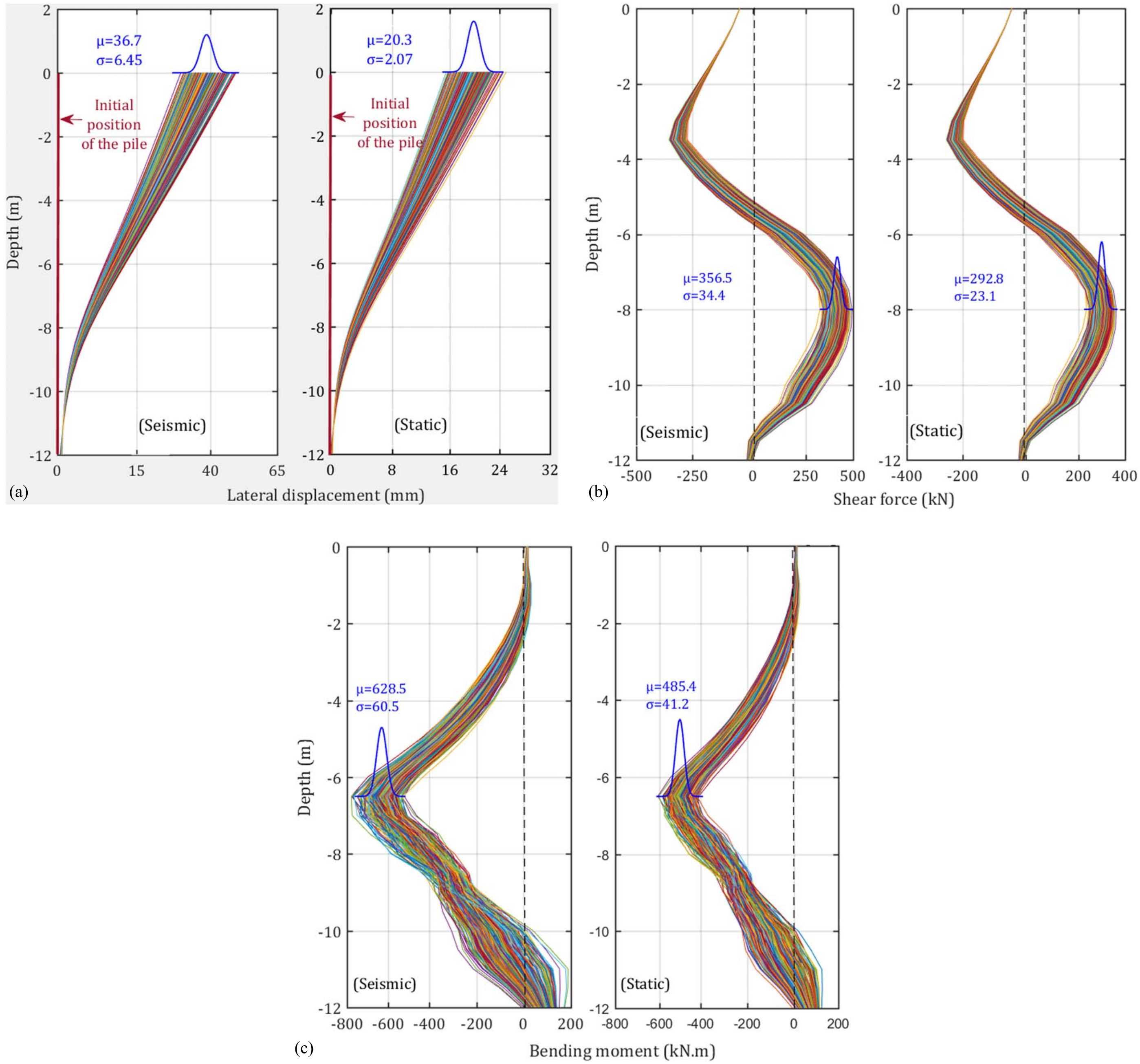

Fig. 13. Variations of soldier piles response for different realizations.

reveals that the conventional URFEM underestimates the β, whereas the CRFEM can efficiently reduce the uncertainties and give more reliable outcomes.

Effects of Conditional Simulation on the Shape and Position of Slip Surfaces

The superiority of the FEM over other stability analysis methods lies in obtaining the slip surface without needing any primary assumption. To investigate the influence of geostatistical conditional simulation on the shape and position of a critical slip surface, 500 realizations are generated using the URFEM and CRFEM in a seismic state. In each simulation, the critical slip surface is recognized by identifying elements with the highest shear strain and fitting a polynomial function through its centers. Figs. 15(a and b) illustrate the shape and position of critical slip surfaces in the URFEM and CRFEM analyses, respectively. It can be seen that by changing the analysis from the URFEM to the CRFEM, the mechanism changes from closely translational to rotational failure, and the rupture surface is indicative of maximum deviatoric plastic strain moving downward. These figures imply that the unsafe zone adjacent to the excavation decreases by using geostatistical conditional simulation. Also, it can be seen that implementing the known data in the stability analysis by using the CRFEM results in less extensive failure zones and a lower σ, which implies less uncertainty in the slip surfaces.

System Reliability Analysis of Soldier Pile Wall

As mentioned previously, the soldier pile wall system consists of four components (i.e., FS_{BM}, FS_{SF}, FS_{LD}, and FS_G) correlated

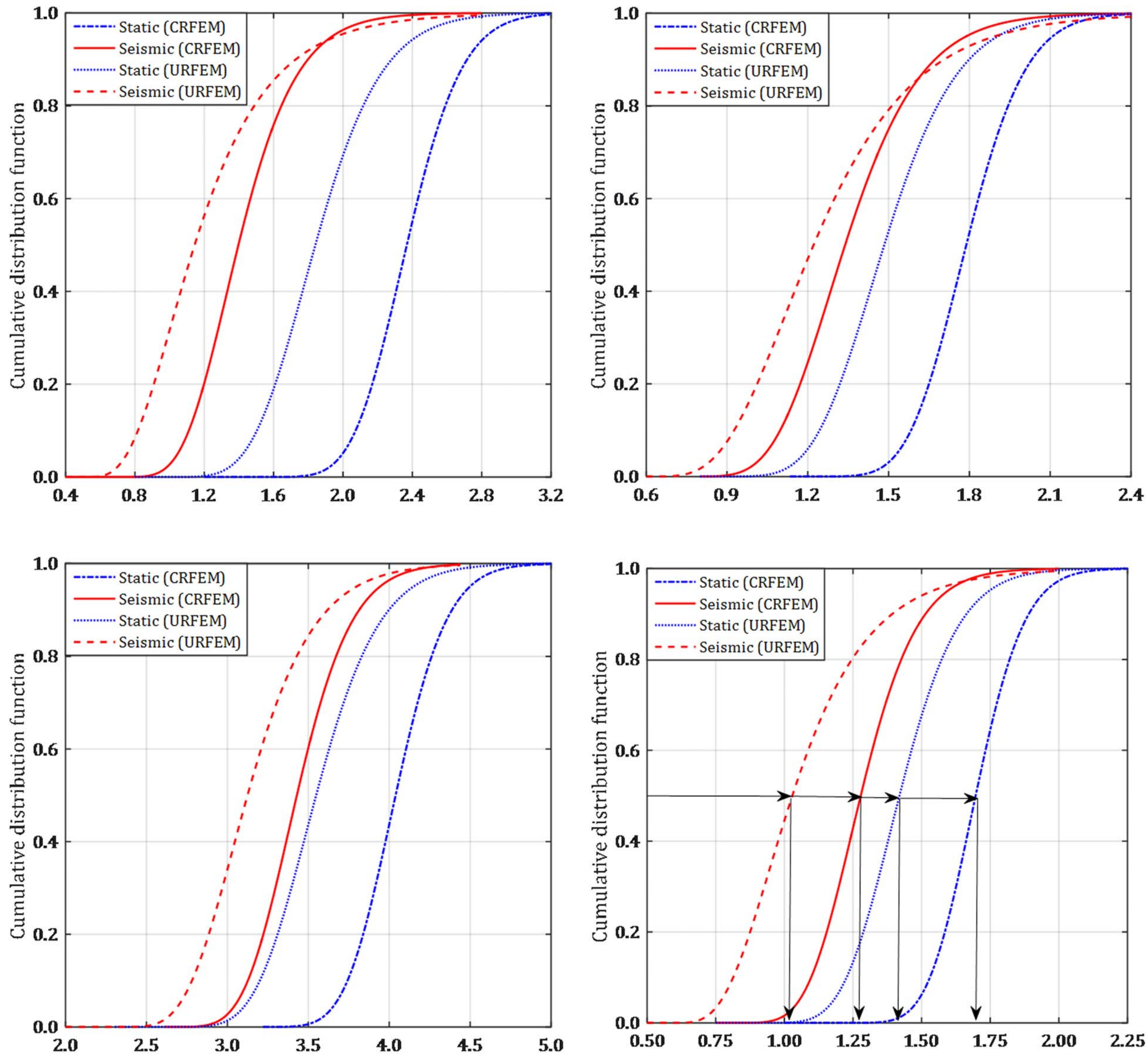

Fig. 14. CDF of (a) FS_{LD}; (b) FS_{SF}; (c) FS_{SF}; and (d) FS_{BM}.

with different dependencies. Hence, a design based on individual failure modes may lead to an unreliable design. The main advantage of the system reliability analysis is that it offers overall system reliability instead of several individual reliability indices (Johari et al. 2021). The SCM is selected and implemented in the case study among various methods developed so far to extract overall system reliability. In this method, which is one of the most popular ones due to its simplicity and good performance, the components' reliability is first obtained. The components are subsequently combined into equivalent components two at a time until the system's overall reliability is extracted. Utilizing this method involves the reliability index of the components and the correlation matrix between them.

To obtain the correlation matrix, the correlation between the FSs of two failure modes was selected as a correlation coefficient of them (Johari and Kalantari 2021). This procedure was repeated to extract the global correlation matrix, Eqs. (13) and (14) for the CRFEM analysis in the static and seismic state, respectively. The procedure of extracting the system reliability index of the soldier pile wall for the CRFEM analysis is presented in Figs. 16(a and b), respectively, for the static and seismic conditions. It is observed that by considering the seismic conditions, the overall reliability index decreases from 4.83 to 1.59, or in other words, the performance level dips from high to unsatisfactory (USACE 1997).

$$\boldsymbol{\rho}_{Static} = \left[\begin{array}{ccccc} FS_{BM} & FS_{SF} & FS_{LD} & FS_{G} & \\ 1 & 0.79 & 0.66 & 0.69 & FS_{BM} \\ & 1 & 0.59 & 0.73 & FS_{SF} \\ & & 1 & 0.51 & FS_{LD} \\ sym. & & & 1 & FS_{G} \end{array}\right] \quad (13)$$

Int. J. Geomech., 2022, 22(10): 04022159

Table 11. Statistical parameters of all failure modes for different conditions

Condition	Analysis type	Failure mode	μ	σ	β	COV (%)
Static	CRFEM	FS_{BM}	1.74	0.16	4.83	0.08
		FS_{SF}	4.08	0.27	12.32	0.07
		FS_{LD}	2.43	0.26	5.52	0.11
		FS_G	1.91	0.17	5.71	0.09
	URFEM	FS_{BM}	1.47	0.17	2.95	0.12
		FS_{SF}	3.71	0.30	9.28	0.08
		FS_{LD}	1.88	0.28	3.31	0.15
		FS_G	1.62	0.19	3.42	0.12
Seismic	CRFEM	FS_{BM}	1.32	0.18	2.03	0.14
		FS_{SF}	3.47	0.26	9.72	0.07
		FS_{LD}	1.45	0.27	1.81	0.19
		FS_G	1.41	0.19	2.28	0.13
	URFEM	FS_{BM}	1.12	0.22	0.80	0.20
		FS_{SF}	3.23	0.33	6.94	0.10
		FS_{LD}	1.11	0.35	0.37	0.31
		FS_G	1.22	0.28	0.86	0.23

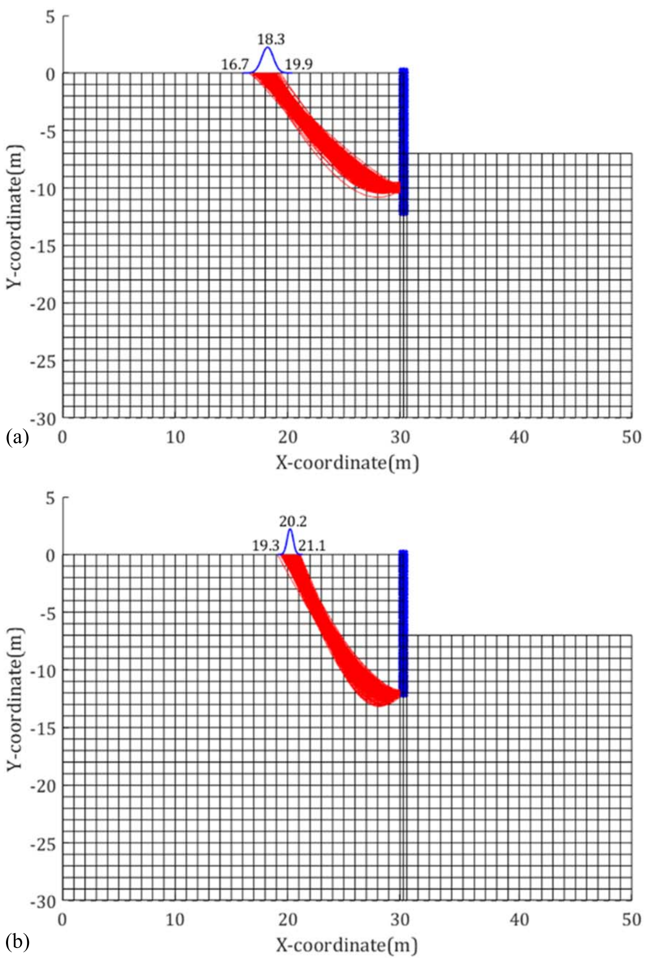

Fig. 15. Slip surface uncertainties of the soldier pile wall in the seismic state of (a) URFEM analysis; and (b) CRFEM analysis.

$$\rho_{Seismic} = \begin{array}{c} \\ \left[\begin{array}{ccccc} FS_{BM} & FS_{SF} & FS_{LD} & FS_G & \\ 1 & 0.81 & 0.64 & 0.72 & FS_{BM} \\ & 1 & 0.60 & 0.78 & FS_{SF} \\ & & 1 & 0.57 & FS_{LD} \\ sym. & & & 1 & FS_G \end{array} \right] \end{array} \quad (14)$$

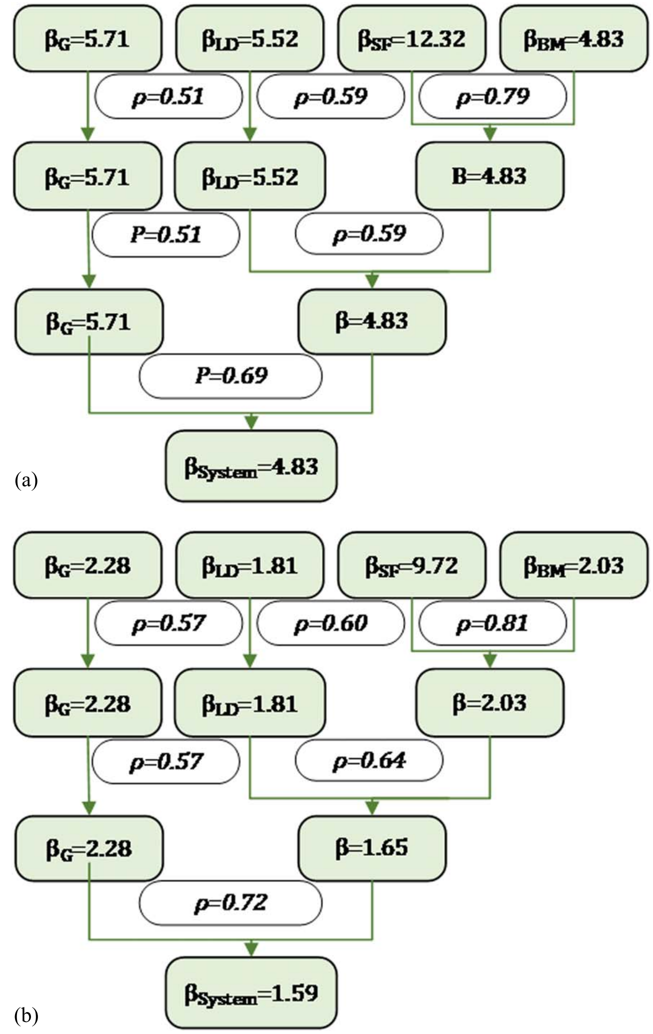

Fig. 16. Procedure for determining the soldier pile wall system reliability index: (a) static state; and (b) seismic state.

Conclusions and Recommendations

This article presents the seismic system reliability analysis of the soldier pile wall by considering different failure modes and the uncertainty associated with soil parameters and the seismic coefficient. The need to develop such a methodology was felt due to the lack of literature on the seismic reliability analysis of soldier piled excavation. The structural and geotechnical limit states, system reliability analysis, conditional simulation, cross-correlation between multiple failure modes, and uncertainty of soil properties and the seismic coefficient were all considered in the methodology. To the best of the authors' knowledge, no study that performs the system reliability analysis of soldier piled excavation considering both the geotechnical and the structural limit states together in a pseudostatic finite-element framework is available to date. For this analysis, a real case with three boreholes of 22.5- m depth was selected, and the soil parameters were extracted based on laboratory and field measurements. The pseudostatic analysis was performed deterministically using a finite-element-based program coded in MATLAB 2015(b). Then, the stochastic analysis was conducted using the URFEM and CRFEM to consider the seismic coefficient and soil heterogeneity. Finally, the reliability indices of different failure modes were obtained, and the overall reliability index was calculated using the SCM. According to the results, several conclusions can be drawn and summarized as follows:

1. The results of sensitivity analysis for determining the model's dimensions revealed that the optimum length and height of the model was approximately 2.5 and 4 times the soldier pile length.
2. The sensitivity analysis for reliability assessment illustrated that the required number of realizations was 500. Also, it was found that in addition to the k_h, which played a crucial role in the seismic stability of the retaining system, the γ, c, φ, and E_S were the effective soil parameters.
3. An assessment of the responses of soldier piles indicated that by taking the seismic state into account, the mean value of maximum lateral displacement, shear force, and bending moment increased to 80%, 16%, and 37%, respectively. Besides, the related standard deviation increased by 3.11, 1.32, and 2.25 times, respectively, which changed the performance level of the stability condition.
4. An evaluation of the COV of CDFs indicated that in both static and seismic states, the effect of soil heterogeneity on FS_{LD} was high relative to others, while FS_{SF} was less influenced compared with the others.
5. From the CDF of the FS concerning all failure modes in the seismic state, it was illustrated that utilizing the conditional simulation will increase the mean value of the FS in terms of lateral displacement, shear force, bending moment, and global stability by 30.6%, 7.4%, 17.9%, and 15.6%, respectively. Also, it was found that considering the known data into the model decreased the standard deviations of the FS concerning lateral displacement, shear force, bending moment, and global stability by 22.9%, 21.2%, 18.2%, and 32.1%, respectively, which could be counted as a goal of reliability analysis.
6. Implementing the known data in stability analysis using conditional simulation resulted in lower uncertainty of the slip surface and less extensive failure wedge that reduced the unsafe zone from the edge of the excavation by 16.2%.
7. The extracted correlation matrix for system reliability analysis, which showed the dependency of failure modes, revealed that the FS_{SF} and FS_{BM} were mutually dependent on each other in static and seismic conditions.
8. A separate consideration of different failure modes led to an overestimation of the reliability indices by three times. Also, the results indicated that bending moment and lateral displacement were the key mechanisms in the static and seismic states.
9. The good lognormal fits were obtained for the CDF of the FS concerning all failure modes despite normal probability distribution for random variables.

The proposed method evaluated the stochastic behavior of soldier-piled excavation in a seismic state, but the effect of duration, frequency of earthquake, amplification effects, and phase change in shear and primary waves propagating in the backfill behind the retaining wall was not considered. Hence, further research is required to compare the seismic stability of soldier piled walls under pseudostatic, pseudodynamic, and dynamic conditions.

Data Availability Statement

All data, models, or code generated or used during the study are available from the corresponding author by request.

References

Ali, J., and A. Q. Khan. 2017. "Behaviour of anchored pile wall excavations in clays." *Proc. Inst. Civ. Eng. Geotech. Eng.* 170 (6): 493–502. https://doi.org/10.1680/jgeen.16.00071.

Basha, B. M., and G. S. Babu. 2009. "Reliability based design optimization for internal stability of reinforced soil structures using pseudo-static method." In *Contemporary Topics in In Situ Testing, Analysis, and Reliability of Foundations*, Geotechnical Special Publication 186, edited by M. Iskander, D. F. Laefer, and M. H. Hussein, 364–371. Reston, VA: ASCE.

Bathurst, R. J., and Z. Cai. 1995. "Pseudo-static seismic analysis of geosynthetic-reinforced segmental retaining walls." *Geosynth. Int.* 2 (5): 787–830. https://doi.org/10.1680/gein.2.0037.

Behpoor, L., and A. Ghahramani. 1989. "Correlation of SPT to strength and modulus of elasticity of cohesive soils." In *12th Int. Conf. on Soil Mechanics and Foundation Engineering*. Rotterdam, Netherlands: A. A. Balkema.

BHRC (Building and Housing Research Center). 2014a. *Iranian code of practice for soil mechanics, design and execution of foundations*. 3rd ed. Standard No. 7. Tehran, Iran: BHRC.

BHRC (Building and Housing Research Center). 2014b. *Iranian code of practice for seismic resistant design of buildings*. 4th ed. Standard No. 2800. Tehran, Iran: BHRC.

Bowles, J. E. 1988. *Foundation analysis and design*. 5th ed. Singapore: McGrawHill.

Bray, J. D., T. Travasarou, and J. Zupan. 2010. "Seismic displacement design of earth retaining structures." In *Proc. 3rd Earth Retention Conf.* 638–655. Reston, VA: ASCE.

Brinkgreve, R., S. Kumarswamy, W. Swolfs, D. Waterman, A. Chesaru, and P. Bonnier. 2014. *Plaxis 2014*. Delft, Netherlands: Plaxis.

CEN (European Committee for Standardization). 2005. *Design of structures for earthquake resistance*. Part 1:1998–1991. Eurocode 8. Brussels, Belgium: CEN.

Cherubini, C. 2000. "Reliability evaluation of shallow foundation bearing capacity on $c'\varphi'$ soils." *Can. Geotech. J.* 37 (1): 264–269.

Choudhury, D., and S. M. Ahmad. 2007. "Stability of waterfront retaining wall subjected to pseudo-static earthquake forces." *Ocean Eng.* 34 (14–15): 1947–1954. https://doi.org/10.1016/j.oceaneng.2007.03.005.

Estes, A. C., and D. M. Frangopol. 1998. "RELSYS: A computer program for structural system reliability." *Struct. Eng. Mech.* 6 (8): 901–919. https://doi.org/10.12989/sem.1998.6.8.901.

Genske, D. D., T. Adachi, and M. Sugito. 1991. "Reliability analysis of reinforced earth retaining structures subjected to earthquake loading." *Soils Found.* 31 (4): 48–60. https://doi.org/10.3208/sandf1972.31.4_48.

Gholampour, A., and A. Johari. 2019. "Reliability-based analysis of braced excavation in unsaturated soils considering conditional spatial variability." *Comput. Geotech.* 115: 103163. https://doi.org/10.1016/j.compgeo.2019.103163.

Griffiths, D. V., and G. A. Fenton. 2007. *Probabilistic methods in geotechnical engineering*. New York: Springer.

GuhaRay, A., and D. K. Baidya. 2016. "Reliability coupled sensitivity-based seismic analysis of gravity retaining wall using pseudostatic approach." *J. Geotech. Geoenviron. Eng.* 142 (6): 04016010. https://doi.org/10.1061/(ASCE)GT.1943-5606.0001467.

Hu, H., Y. Huang, and M. Xiong. 2022. "PDEM-based seismic performance assessment of retaining walls considering spatial variability of soil properties." *J. Earthquake Eng.* 26 (1): 52–69.

Johari, A., and H. Fooladi. 2020. "Comparative study of stochastic slope stability analysis based on conditional and unconditional random field." *Comput. Geotech.* 125: 103707. https://doi.org/10.1016/j.compgeo.2020.103707.

Johari, A., and A. R. Kalantari. 2021. "System reliability analysis of soldier-piled excavation in unsaturated soil by combining random finite element and sequential compounding methods." *Bull. Eng. Geol. Environ.* 80 (3): 2485–2507. https://doi.org/10.1007/s10064-020-02022-3.

Johari, A., and H. Rahmati. 2019. "System reliability analysis of slopes based on the method of slices using sequential compounding method."

Comput. Geotech. 114: 103116. https://doi.org/10.1016/j.compgeo.2019.103116.

Johari, A., B. Vali, and H. Golkarfard. 2021. "System reliability analysis of ground response based on peak ground acceleration considering soil layers cross-correlation." *Soil Dyn. Earthquake Eng.* 141: 106475. https://doi.org/10.1016/j.soildyn.2020.106475.

Kang, W.-H., and J. Song. 2010. "Evaluation of multivariate normal integrals for general systems by sequential compounding." *Struct. Saf.* 32 (1): 35–41. https://doi.org/10.1016/j.strusafe.2009.06.001.

Karakostas, C. Z., and G. D. Manolis. 2002. "Dynamic response of tunnels in stochastic soils by the boundary element method." *Eng. Anal. Boundary Elem.* 26 (8): 667–680. https://doi.org/10.1016/S0955-7997(02)00034-6.

Kontoe, S., L. Pelecanos, and D. Potts. 2013. "An important pitfall of pseudo-static finite element analysis." *Comput. Geotech.* 48: 41–50. https://doi.org/10.1016/j.compgeo.2012.09.003.

Li, R., Y. Yu, L. Deng, and G. Li. 2006. "Stability analysis of unsaturated soil slope by 3-D strength reduction FEM." In *Advances in Unsaturated Soil, Seepage, and Environmental Geotechnics*, Geotechnical Special Publication 148, edited by N. Lu, L. R. Hoyos, and L. Reddi, 62–69. Reston, VA: ASCE.

Luo, Z., Y. Li, S. Zhou, and H. Di. 2018. "Effects of vertical spatial variability on supported excavations in sands considering multiple geotechnical and structural failure modes." *Comput. Geotech.* 95: 16–29. https://doi.org/10.1016/j.compgeo.2017.11.017.

Matheron, G. 1963. "Principles of geostatistics." *Econ. Geol.* 58 (8): 1246–1266. https://doi.org/10.2113/gsecongeo.58.8.1246.

Mononobe, N. 1929. "On determination of earth pressure during earthquake." In *Proc., World Engineering Congress*, 177–187. Japan: Kogakkai.

Okabe, S. 1926. "General theory of earth pressure." *J. Jpn*. *Soc*. *Civ*. Eng. 12(1).

Parsons, R., and J. Frost. 2002. "Evaluating site investigation quality using GIS and geostatistics." *J. Geotech. Geoenviron. Eng.* 128 (6): 451–461. https://doi.org/10.1061/(ASCE)1090-0241(2002)128:6(451).

Phoon, K.-K., and F. H. Kulhawy. 1999. "Evaluation of geotechnical property variability." *Can. Geotech. J.* 36 (4): 625–639. https://doi.org/10.1139/t99-039.

Rahman, M., and H. B. K. Nguyen. 2012. *Applications of random finite element method in bearing capacity problems*. In *Proc., ADVCOMP 2012, 6th Int. Conf. on Advanced Engineering Computing and Applications in Sciences*, 53–58. Red Hook, NY: Xpert Publishing Services.

Richards, R., Jr., and D. G. Elms. 1979. "Seismic behavior of gravity retaining walls." *J. Geotech. Geoenviron. Eng.* 105 (GT4): 449–464.

Rouhani, S., R. M. Srivastava, A. J. Desbarats, M. V. Cromer, and A. I. Johnson. 1996. *Geostatistics for environmental and geotechnical applications*. West Conshohocken, PA: ASTM.

Ruan, X., and S. Sun. 2014. "External seismic stability of vertical geosynthetic-reinforced soil walls using pseudo-static method." *Acta Geotech.* 9 (6): 1085–1095. https://doi.org/10.1007/s11440-013-0241-8.

Rushan, L., and S. Hongbin. 2006. "An improved pseudo-static method for seismic resistant design of underground structures." *Earthquake Eng. Eng. Vibr.* 5 (2): 189–193. https://doi.org/10.1007/s11803-006-0586-1.

Seed, H. B., and R. Whitman. 1970. "Design of earth retaining structures for dynamic loads." In *Proc., ASCE Specialty Conf.-Lateral Stress in the Ground and Design of Earth Retaining Structures*, 103–147. Reston, VA: ASCE.

Selvadurai, A., and M. Boulon. 1995. *Mechanics of geomaterial interfaces*. Amsterdam, Netherlands: Elsevier.

Smith, C. C., and M. Cubrinovski. 2011. "Pseudo-static limit analysis by discontinuity layout optimization: Application to seismic analysis of retaining walls." *Soil Dyn. Earthquake Eng.* 31 (10): 1311–1323. https://doi.org/10.1016/j.soildyn.2011.03.014.

Smith, I. M., D. V. Griffiths, and L. Margetts. 2013. *Programming the finite element method*. Hoboken, NJ: Wiley.

Song, J., and W.-H. Kang. 2009. "System reliability and sensitivity under statistical dependence by matrix-based system reliability method." *Struct. Saf.* 31 (2): 148–156. https://doi.org/10.1016/j.strusafe.2008.06.012.

USACE. 1997. *Engineering and design: Introduction to probability and reliability methods for use in geotechnical engineering*. Engineer Technical Letter. Washington, DC: USACE.

Webster, R., and M. A. Oliver. 2007. *Geostatistics for environmental scientists*. Hoboken, NJ: Wiley.

Zou, Y., H. Liu, L. Jing, and J. Cui. 2017. "A pseudo-static method for seismic responses of underground frame structures subjected to increasing excitations." *Tunnelling Underground Space Technol.* 65: 106–120. https://doi.org/10.1016/j.tust.2017.02.006.